RSC Advances

REVIEW

View Article Online
View Journal | View Issue

Cite this: *RSC Adv.*, 2019, **9**, 35566

Synthesis and compatibility evaluation of versatile mesoporous silica nanoparticles with red blood cells: an overview

Subhankar Mukhopadhyay, Hanitrarimalala Veroniaina, Tadious Chimombe, Lidong Han, Wu Zhenghong* and Qi Xiaole*

Received 7th August 2019
Accepted 18th September 2019

DOI: 10.1039/c9ra06127d

rsc.li/rsc-advances

Protean mesoporous silica nanoparticles (MSNs) are propitious candidates over decades for nanoscale drug delivery systems due to their unique characteristics, including (but not limited to) changeable pore size, mesoporosity, high drug loading capacity, and biodegradability. MSNs have been drawing considerable attention as competent, safer and effective drug delivery vehicles day by day by their towering mechanical, chemical and thermal characteristics. Straightforward and easy steps are involved in the synthesis of MSNs at a relatively cheaper cost. This review reports Stober's synthesis, the first proposed synthesis procedure to prepare micron-sized, spherical MSNs, followed by other modifications later on done by scientists. To ensure the safety and compatibility of MSNs with biological systems, the hemocompatibility evaluation of MSNs using human red blood cells (RBCs) is a widely welcomed exercise. Though our main vision of this overview is to emphasize more on the hemocompatibility of MSNs to RBCs, we also brief about the synthesis and widespread applications of multifaceted MSNs. The strike of different parameters of MSNs plays a crucial role concerning the hemolytic activity of MSNs, which also has been discussed here. The inference is derived by centering some feasible measures that can be adopted to cut down or stop the hemolytic activity of MSNs in the future.

1. Introduction

Among natural compounds, silica is aplenty in nature. It has mainly two forms: crystalline and amorphous. The crystalline form of silica is considered as a toxic substance, whereas the amorphous form has been boundlessly used due to its biocompatibility, biodegradability and nontoxicity.[1] Among various types of silica nanoparticles, MSNs with a pore size ranging from 2 to 100 nm are extensively used as nanocarriers in the nanoscale drug delivery systems (NDDSs).[2–4] High drug loading capacity, biodegradability, biocompatibility, ease of surface modification, ease of synthesis, targetability and control over particle and pore sizes and its shape during the synthesis make MSNs promising candidates for a controlled and sustained drug delivery system as nanocarrier, bioimaging, biosensing and theranostic agents.[5–7] Mesoporous materials are more resistant to outer stimuli such as degradation and mechanical stress because of the powerful Si–O bond than their other counterparts (niosomes, liposomes, dendrimers, *etc.*). So, this property is beneficial because of the lack of necessity of outer stabilization during the synthesis of MSNs.[8,9] MSNs, such as MCM-41 and SBA-15, have orderly cylindrical pore structures potentially used in the biomedical discipline. Small molecules, small drugs, antibiotics, antibodies, and therapeutic proteins can be delivered *via* MSNs due to their colossal pore volume, large surface area and adjustable pore size.[10] In the 1990s, Kresge *et al.* and Yanagisawa *et al.* first published their paper on mesoporous (Fig. 1) materials.[11]

Hemocompatibility is mainly an *in vitro* test performed to evaluate the chances of a test sample to cause unfavorable effects on red blood cells (hemolysis), coagulation, thrombosis, platelets and complement systems. To accomplish the desired results, sample nanomaterials need to come in direct contact with cells and tissues. Therefore, the safe use of nanomaterials towards cells and tissues is the main concern nowadays in the nanodrug delivery system. RBCs are the first component in blood coming into direct contact with nanomaterials because of its size and administration route. If the adverse effect takes place among circulating red blood cells, there will be no meaning of sending nanomaterials capable of freeing up pharmaceutical ingredients on demand.

The hemolytic activity of nanomaterials can be well evaluated by the proposed method of the American Society for Testing and Materials (ASTM) (in 2008). The main goal of this standard test method is to evaluate the percentage of hemoglobin (Hb) released when nanocarriers come in direct contact with RBC surfaces and at this moment cause cell lysis. It is important to check the hemocompatibility of any nanomaterial before its use. The above

Key Laboratory of Modern Chinese Medicines, China Pharmaceutical University, Nanjing 210009, PR China. E-mail: zhenghongwu66@cpu.edu.cn; qixiaole523@cpu.edu.cn; Fax: +86-025-83179703; Tel: +86-15062208341

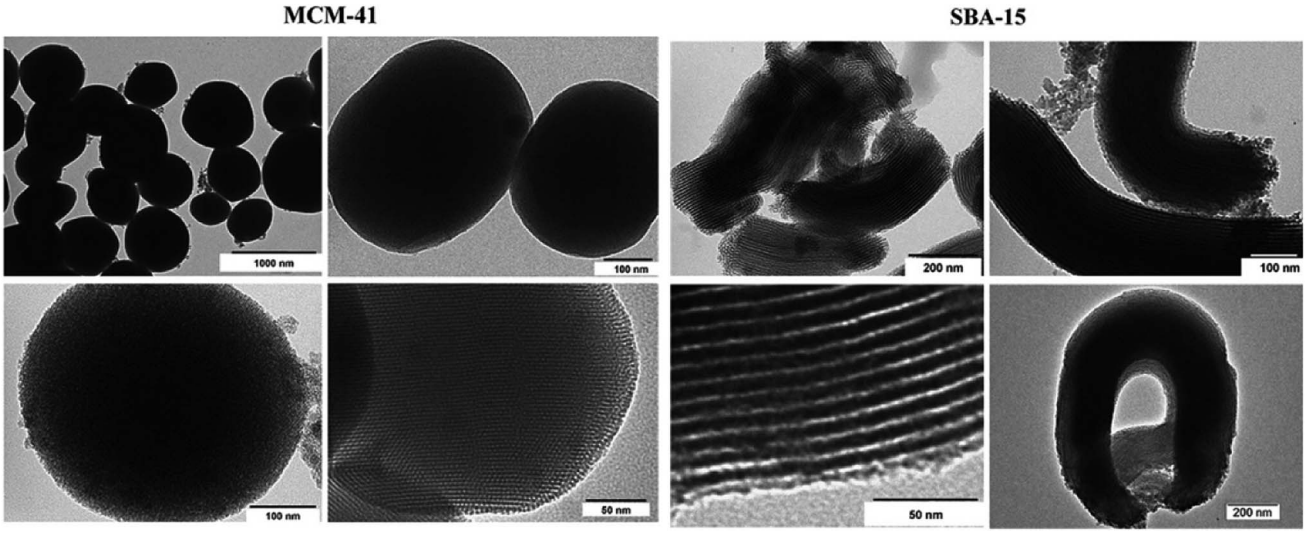

Fig. 1 TEM image of MCM-41 and SBA-15. Reprinted with permission from ref. 12. Copyright © 2008, American Chemical Society.

proposed hemolytic test is very much acceptable to access the hemocompatibility of nanomaterials on account of their low cost, biodegradability and prompt results.[6,13] As MSNs are essential candidates in the biomedical field, it is indispensable to acquire ample data about their viable hemocompatibility and the parameters responsible for interfering the hemocompatibility to ensure effective and biocompatible drug delivery.[10]

2. Synthesis of MSNs

As well known, "Stober synthesis" is the former chemical method by which Stober successfully achieved globular monodisperse micrometer-sized silica particles.[14] According to the name of the scientist, the synthetic process for the development of MSNs was recognized as Stober's synthesis. Numerous remodeling and improvements have been persistently carried out towards the aforementioned method to get orderly arranged, monodisperse, nanometer-sized MSNs. Different changes and modifications can be done to the reaction conditions to obtain MSNs with altering appearance and dimensions. Grün *et al.* first successfully prepared spherical-shaped MCM-41 (Mobil Crystalline Matter) after modifying Stober's proposed method.[15] Before that only hexagonal MCM-41 type was available. Continuous improvement in this research arena further helps to yield fixed, properly arranged MSNs.

Consistent pore size and high pore volume than expected make MSNs interesting nanocarriers for novel drug delivery systems. Those listed characters can be restrained by altering the temperature, surface-active agent's concentration, sources of silica and pH of the reaction media. Liquid crystal pattern process is the mechanism through which the precipitation of silica takes place on the outer layer of surfactant micelles, yielding solid silica.[16–18]

2.1. Mechanisms involved in the formation of MSNs

A piece of proper knowledge on the procedure of the production of MSNs is essential to obtain nanoparticles with required characteristics for a novel drug delivery system. The formerly mentioned mechanism stated that silica web formed all around the non-ionic surface-active agent's liquid-crystalline stages. This is correct for particles obtained from the dilution of surface-active agents, but no systemic mesoporous particles were found.[19] The research works demonstrated two processes one of them is the adsorption of hydrolyzed MCM-41 onto the surface of the micelles and other one is for SBA-15 (Santa Barbara Amorphous) where at primary step the reaction between surface-active agent and silica occurs which further leads to the generation of core shell-like edifice.[20] Fig. 2 demonstrates the mechanism involved in the formation of MCM-41. However, now, many scientists are working to understand the exact mechanism underlying the production of MSNs.

Time-resolved small-angle neutron scattering (SANS) is an *in situ* technique to determine the production of MSNs, which helps to understand simultaneous changes in the formation mechanism. A cluster of small silica particles were obtained during the initial hydrolysis (~40 s) of tetramethyl orthosilicate (TMOS). In the growth stage, the adsorption of the silicate ion onto the surface of the surface-active agent micelles occurs. At the primary hydrolysis stage, surfactant's surrounding charge lowers, which further reduces intermicellar repulsive force and accumulates silica particles. Hexagonally well-ordered MSNs were abundantly present in the reaction mixture after ~400 s and this was ensured after transmission electron microscopic (TEM) evaluation.[23,24]

2.1.1. Swelling–shrinking mechanism. "Swelling–shrinking mechanism" is a procedure to prepare MSNs, and this evaluates its characteristics by adapting time-resolved synchrotron small-angle X-ray scattering (SAXS). When tetraethyl orthosilicate (TEOS) is independently adapted as a forerunner and any other solvent, for example, ethanol is not present, the above-mentioned mechanism works well. TEOS is an oily tetrahedral ethyl ester of orthosilicic acid that demonstrated phase separation under steady conditions, but in case of forceful stirring, it forms an emulsion complex.

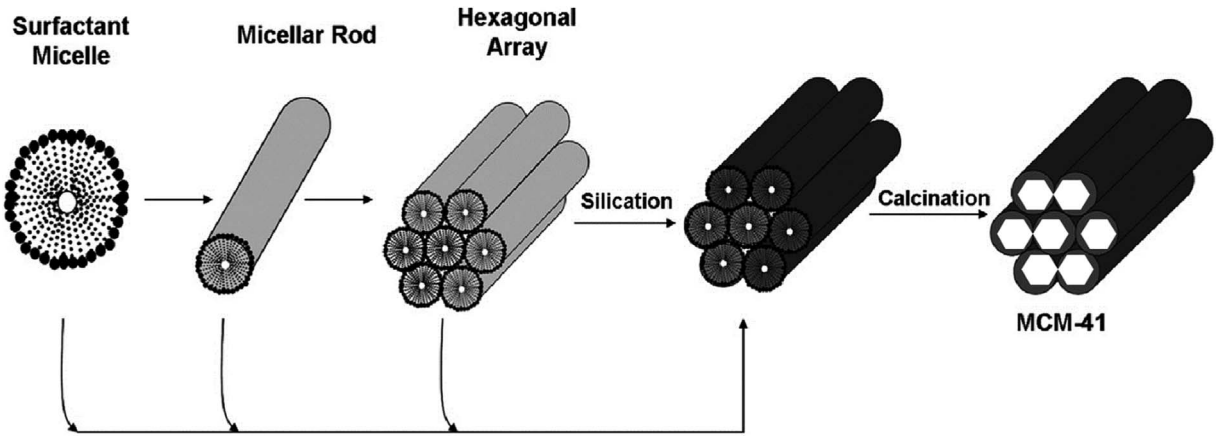

Fig. 2 Proposed LCT (liquid crystal templating) synthetic mechanism to form MCM-41 (ref. 21 and 22). Two pathways are involved during the synthesis process, as described earlier. Reprinted from ref. 22. Copyright © 1992 American Chemical Society.

Cetyltrimethylammonium bromide (CTAB) was first used as a template to build well-ordered mesoporous materials. It forms ellipsoidal micelles that have an inner hydrophobic tail core. Spherical micelles were formed after the addition of TEOS, which helped to dissolve CTAB in the hydrophobic core and enlarge the micelles. Upon the hydrolysis of TEOS, monomers are prone to be hydrophilic and they free-up into the surrounding aqueous environment. Electrostatic attraction plays an important role to adsorb negatively charged hydrolyzed monomers of TEOS to the positively charged CTAB micelles. The total ingestion of TEOS into the hydrophobic core leads to the formation of wrinkled and lesser-sized micelles. The two critical operations, namely, hydrolysis and condensation take place at the same time in this process. This effect brought shrunken micelles until complete TEOS hydrolysis and silica shell formation throughout the micelles. Finally, the aggregation of the adjacent micelles occurs and the growth of the particle and mesostructure is observed.[25]

2.1.2. Sol–gel technique. "Sol–gel technique" is mainly the modification of Stober's proposed process, which is widely used to fabricate MSNs. It is more prevalent among scientists and researchers than other mechanisms. Extensive research has been done according to this method to synthesize inorganic materials. According to this process, alkoxide monomers are adapted as precursors that get hydrolyzed and condensed into the colloidal mixture (sol). After hydrolysis and condensation, it forms a well-ordered network (gel) of polymers or distinct particles. Acid or base catalysts have a high impact on the "sol–gel technique". Two factors influence the hydrolysis of alkoxide groups: one is the state of the reaction and another is the Si/H_2O molar ratio. Basic environment increases the hydrolysis rate than the acidic counterpart. The hydrolysis phase is very crucial because that determines the rate of condensation in the future. After condensation, in many cases, it is observed that the chain-like structure presented in sol form and the network-like structure in gel form.[26]

2.2. Basic employed components

The main components that respond to form the core of MSNs are the silica precursor, catalyst and surfactant along with other adjuvants, such as pore-expanders, co-solvents, and aggregation-prevention agents, based on necessity.

2.2.1. Silica precursor. Silica is found in copious amounts on the Earth surface. It can be obtained in two different forms: amorphous and crystalline. Crystalline forms of silica are present in feldspars, zeolites, micas, *etc.*, whereas amorphous forms are abundant in volcanic rocks, ashes, *etc.* Ocean plates show a significant amount of silica source in the form of diatomaceous earth. Inorganic silica sources, including tetraethyl orthosilicate (TEOS),[27,28] tetramethoxysilane (TMOS),[29,30] tetrakis(2-hydroxyethyl)orthosilicate (THEOS),[31] and trimethoxyvinylsilane (TMVS)[32] are generally adopted silica precursors. Thiol-containing precursors such as (3-mercaptopropyl)trimethoxysilane (MPMS) and (3-mercaptopropyl)methyldimethoxysilane (MPDMS) are also used to fabricate organosilica nanoparticles.[33] Bis(triethoxysilyl propyl)disulfide (BTEPDS, $(H_5C_2O)_3Si–(CH_2)_3–S–S–(CH_2)_3–Si(OC_2H_5)_3$) or bis(trimethoxysilyl propyl)disulfide (BTMPDS, $(H_3CO)_3Si–(CH_2)_3–S–S–(CH_2)_3–Si(OCH_3)_3$) and bis(3-triethoxysilyl propyl)tetrasulfide (BTEPTS, $(H_5C_2O)_3Si–(CH_2)_3–S–S–S–S–(CH_2)_3–Si(OC_2H_5)_3$) are two disulfide-bridged silanes available in the market to synthesize disulfide-bridged organosilica skeletons *via* the single-step co-condensation of BTEPTS and TEOS.[34] Bis(triethoxysilyl)ethane (BTEE, $–CH_2–CH_2–$) is also employed as an organosilica source.[35] (3-Aminopropyl)trimethoxysilane (APTMS) and (3-aminopropyl)triethoxysilane (APTES) are also considered as organofunctional alkoxysilane precursors.[36]

2.2.2. Surfactant. One of the most critical components for the synthesis of MSNs is a surfactant. The surfactant moderates and determines the pore size of the formed nanoparticle, which is why they are also known as surface-directing agents or templates. Surfactants or surface-active agents are composed of two distinct structures (hydrophilic and hydrophobic) with the propensity to adsorb at the surface of the particle. They are differentiated in four groups according to their polar head charge, for example, anionic with negatively charged polar head, cationic with positively charged polar head, non-ionic with polyether or polyhydroxyl unit as the polar group and zwitterionic with the neutral charge on their head group.[37]

Commonly used surfactants for the preparation of 2-D hexagonal structures (MCM-41) are cetyltrimethylammonium bromide (CTAB)[27,28] and Pluronic P123 for cubic and hexagonal structures. Surface active agents with the structure $(EO)_x$–$(PO)_y$–$(EO)_x$ (x value ranges from 17 to 37) have been employed to get more hydrothermally stable, thick-walled SBA-15 materials. Some other surfactants are also used frequently, for instance, cetyltrimethylammonium chloride (CTAC),[38,39] Brj-76,[40,41] Tween (20, 40, 60, and 80)[42], Pluronic (F123, F127)[43], Triton (X-100),[44,45] *etc.*

2.2.3. Catalysts. In most of the chemical reactions, catalysts play a vital role to increase the rate of the reaction without itself undergoing any permanent chemical alteration. Many organic amines, including ammonia, are frequently used to impart basic condition during the synthesis of MSNs. Both acidic and basic catalysts are adopted during the synthesis as per the requirements. Other than sodium hydroxide (NaOH) and ammonium hydroxide (NH_4OH), triethanolamine (TEA)[38] was taken as an alternative to produce 20–150 nm sized MSNs. An increasing amount of TEA results in the formation of smaller sized MSNs. TEA acts both as a complexing agent (silicate species) and as a growth inhibitor for MSNs. It also helps to reduce the aggregation of particles. Diethanolamine (DEA),[38,39] hydrogen chloride,[46,47] hydrogen fluoride,[46] and arginine are a few other examples of widely adopted catalysts.

2.2.4. Pore-expanders. Desired pore size is necessary to deliver drugs or biomolecules. Nanoparticles with larger pore sizes can hold a maximum amount of therapeutic agents.[48] Though it is quite challenging to alter the pore size during synthesis, still there are some agents that enlarge the pore of MSNs. Those agents are known as pore-enlarging agents or pore-expanders. *N*,*N*-Dimethylhexadecylamine (DHMA)[49] and 1,3,5-trimethylbenzene (TMB)[50] are applied to cause swelling during the synthesis of MSNs to finally yield pore-expanded MSNs. Some other scientists employed TMB as a pore-enlarging agent to deliver a vast quantity of proteins and DNAs. Tetrapropoxysilane (TPOS),[51] triisopropylbenzene (TIPB),[51,52] and non-ionic triblock co-polymers (Pluronic P103) are also frequently used pore-expanding substances. The alkyl chain length of homologous quaternary ammonium surface-active agents can also be altered to maintain the pore size of synthesized MSNs.

Co-solvents, aggregation-preventers, and reaction media are also demanded as much as the parameters discussed earlier. Water and alcohols (methanol and ethanol)[47] are considered as very good co-solvents. Trihydroxysilylpropylmethyl phosphate[53] works as an interplace aggregation-preventer and disodium hydrogen phosphate[54] as a reaction medium. Few other compounds are also employed according to the reaction condition.

3. Application of MSNs in biological means

As mentioned before, MSNs can be potentially utilized as nanocarriers or drug delivery vehicles for different types of pharmaceuticals and bioactive molecules such as anticancer drugs, nucleotides, and proteins. It is possible because of its unique characteristics. Larger than expected pore size, less hazard to surface modification, and unique mesostructure make MSNs potent carriers to hold and adsorb large quantity of many biomolecules. Easily tunable dimensions of MSNs (60–1000 nm) also make them passive delivery agents for several drugs. Varieties of MSNs with determined surface characteristics and proper dosages may not cause harm to the cells and tissues.[54–58] Extensive research is under pipeline to make MSNs safe and effective nanocarriers. Numerous research and review articles have already discussed the different potential effects of MSNs and their use as nanocarriers for many drugs, biosensors, theranostic agents, bioimaging agents and (Fig. 3) biocatalysts.[55,58]

4. Hemolysis and hemocompatibility

Hemolysis is mainly defined as the destruction of RBCs. There are a lot of factors responsible for the hemolytic or toxic effect of MSNs. Nanoparticle shape, size, surface charge, surface modification, and surface roughness play a crucial role in

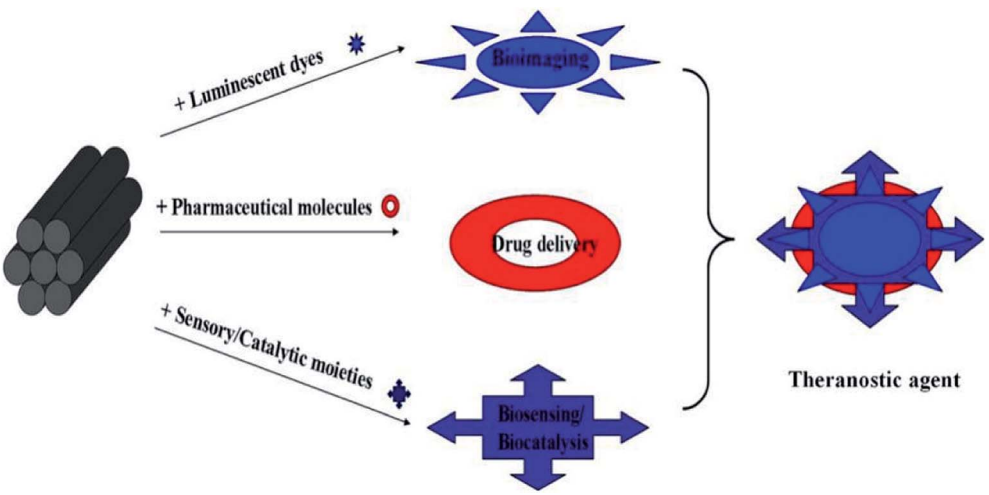

Fig. 3 Different applications of MSNs. Represented with permission from ref. 10. Copyright © 2012 American Chemical Society.

hemocompatibility of MSNs. A diverse range of research has been conducted to modify the hallmarks of MSNs for biological applications. Many *in vivo* and *in vitro* studies have been performed in animal models and tissues, but until now no clinical research was done in human with MSNs.[10,59]

4.1. Evaluation of hemocompatibility

There are several methods available to estimate the hemocompatibility of MSNs with RBCs. Few of them are listed below (Fig. 4).

4.1.1. MSN incubation with human RBCs. *In vitro* model is much more precise to evaluate and quantify the hemocompatibility of biomaterials such as MSNs with sufficient amount of newly collected human blood. *In vitro* model is considered better than *in vivo* model because in the *in vitro* model, we can achieve a restraint overflow rate of blood, prevent coagulation and reduce many hazardous parameters.[60] Up to date, there are not many documents that can assure the actual mechanism of the reaction of MSNs with RBCs and about the resultant product. Nowadays, innumerable devices are available in the market that can be employed to evaluate the hemocompatibility in an *in vitro* model at a pre-determined state. Thereafter, it will assist in contrasting the results straightly. According to Ferrer *et al.*,[61] positive and negative controls need to be tested concurrently for the evaluation of hemocompatibility.

Freshly collected human blood is taken for incubation with MSNs to detect the hemolysis effect. The blood should be high in grade and standard. Blok *et al.*,[62] stated that for the evaluation study, healthy volunteers should be chosen to collect blood. The experiment should start as soon as possible because if the collected blood is kept for more than 4 h, it may hamper the reasonable workability of platelets and leukocytes. The donor should be healthy and physically fit, non-smoker, without pregnancy and not under any medication. Some group of medicines influence the hemostasis process. The blood collection is generally done from the outer vein.

In this study, blood is collected and less quantity of heparin is added to it to prevent coagulation. Three different models such as static, dynamic and agitated are used for the incubation with the sample biomaterial (MSNs) at 37 °C. Activation markers should be examined before and after the incubation process. The MSN surface is a key parameter to determine the interactions between blood proteins and cells with its surface. All the undesired substances, such as by-products, cell debris, solvents, and chemical leftover, should be cleaned and appropriately removed to reduce unwanted effects.[63]

4.1.1.1. Static models. Static blood incubation models are the very handy and fast procedure to evaluate the thrombogenicity. In this simple process in the absence of flow conditions, biomaterials are incubated with blood or plasma where the amount of platelet is high[64] in tubes or well plates. Major drawbacks of this system are the agglomeration of proteins and activation of platelets because this method only gives us elementary level outcomes related to hemocompatibility.[65] Other problems regarding this model are the sedimentation of cells and large blood–air interfaces.

4.1.1.2. Agitated models. In this incubation models, biomaterials such as MSNs are incubated with blood in a flat incubation chamber attached with a shaker or a rotator in the absence of aimed flow.[66] The continuous rotation of the vessels filled with blood and nanoparticles are ensured to stop the precipitation of the test nanomaterials.[67] The primary outcomes of this model are less blood and air contact and lower settling down of cells at the bottom of the container.

4.1.1.3. Shear flow models. Shear flow models are another kind of incubation process to evaluate the hemocompatibility of biomaterials. Interactions take place among nanoparticles and blood when vascular blood circulation imitated.[68] There are many systems involved in *in vitro* shear flow models, which are summarized in Table 1.

4.1.2. Blood cell numbers and hemolysis calculation. A hematology analyzer was used to detect the number of leukocytes, platelets and erythrocytes before and after the incubation period. In thrombogenic materials, the platelet number declines over time and the breakdown of RBCs is called hemolysis. So, erythrocyte damage can be figured out from the inclined concentration of free hemoglobin in plasma[83] (Eva. MSN Hema). A higher amount of free RBCs caused cell toxicity, hampered reasonable kidney activity and lowered the oxygen transport capacity of the destructed RBCs observed in organs and tissues.[84] Microvesicles obtained from RBCs help to form a thrombus in a tissue factor (TF)-based pattern.[85] In some cases, to evaluate hemocompatibility, the biomaterial is directly incubated with blood and in some other cases, the biomaterial extract is used to incubate.[86] The photometric and colorimetric tests are widely accepted methods to determine the hemolysis of a biomaterial. This experiment is performed by adding cyanmethemoglobin (CMH) reagent, which further changes hemoglobin to cyano-derivatives.[87] Based on hemolysis, materials that show 5% hemolysis are defined as hemolytic, in the range between 5 and 2% as slightly hemolytic and under 2% as non-hemolytic materials.[88]

4.1.3. Deformability index. Deformability Index (D.I.) is a parameter by which the deformability of RBCs is calculated. The deformability of RBCs can be defined as the changes in the shape of erythrocytes without hemolysis under certain conditions such as external stress. Various studies already stated that to achieve sustainable drug release and increase the circulation period, the entangling of nanoparticles to the outer surface of

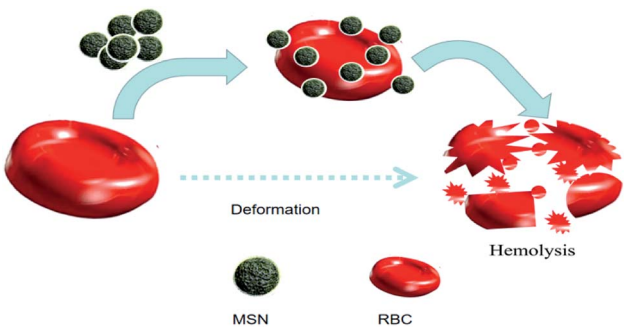

Fig. 4 Hemolysis of RBC after interaction with bare MSNs.

RBCs is essential.[89] Zhao *et al.*, first defined that this type of attachment sometimes causes membrane deformability and hampers the usual workability of RBCs. RBCs with particle sizes ranging between 6 and 8 μm undergo certain deformation to cross the capillaries of the microvascular system. This kind of deformability of RBCs is vital to continue the blood flow that depends on the elasticity of the cell membrane. That is why it is vital to know much more about how MSN attachment causes deformation on RBC membranes.

According to their study, they have used a previously demonstrated filtration method of RBCs *via* polycarbonated membranes.[90] This method is used to determine the deformation of RBCs. First, they incubated fresh human RBCs with different concentrations of MSNs and therefore did the filtration after creating a persistent negative pressure. According to the quantity (ml) of RBCs filtered per minute, the DI was calculated. The time consumed by every RBC suspension to pass through the membrane was also recorded. Fig. 5 shows that if the MSN concentration inclined, then the deformation of RBCs declined.

As shown in Fig. 5, l-MSNs at shallow concentration caused significant damages to RBCs. As per the study, surface-modified (AP and PEG) s-MSNs exhibit better flexibility to RBCs rather than s-MSNs without any modification and CA-s-MSNs (higher concentration). The outcome said that MSN attachment to the outer surface of RBCs causes deformability problems and restrains the elasticity of RBCs. The surface modification of MSNs restricts the contact between particles and membranes. Thus, it gives a green signal to the RBCs to maintain their deformability.

4.2. Impact of different kinds of parameters on the hemocompatibility of MSNs

4.2.1. Particle size. The particle size always elucidates its role to ensure the hemocompatibility or toxicity of MSNs. Lin *et al.* demonstrated the hemolytic effect of MSNs in RBCs using the hemolytic assay.[27] They had taken a varied size range of MSNs (25 to 225 nm) to conduct the test. In the final outcome, MSNs showed size- and dose-dependent hemolysis on RBCs (exception of the smallest MSNs). Hemolytic activity on RBCs is directly proportional to the diameter of the MSNs. MSN-25 demonstrates as a low hemolytic active compound because of their bigger-than-presumed pore size and huge primary pore volume when contrasted with large diameter MSNs.

Table 1 Summary of different types of shear-flow models to evaluate hemolysis

System	Mechanism	Ref.
Flat plate flow chamber	This chamber consists of a flat piece of biomaterial and parallel-plate viscometers. Blood flows over them To minimize sedimentation, aliquot of blood is gently mixed for 60 seconds	69
Parallel and cone plated viscometer	Blood circulation happens between two parallel-fitted biomaterials (MSNs) built plate. One plate revolves over another Here, dynamic interaction occurs between biomaterial and blood. Rotating cone and plate used as a shear stress source	70
"Chandler loop" (tubular systems)	A biomaterial coated round-shaped channel containing air bubble-blood is revolved at 37 °C to ignite blood flow	71–73
Modified chandler loop	Blood filled after tube or conduit fitted with stents	74
Blood-endothelial cell chamber model and microfluidic flow model	In a blood endothelial cell chamber model, biomaterial interactions with whole blood and endothelium checked where in addition, microfluidics can be implemented to judge the platelet and coagulation activation Here, the outer face of the incubation chamber that contacted with blood were seeded with human umbilical vein endothelial cells (HUVECs)	75–81
Hemobile model	In this model, no mechanical implements involve compressing the tubing. Unidirectional circulation achieved due to the presence of a one-way ball valve. Also, the pipe is free of air	82
Roller pump closed-loop test systems	This system has undertaken to overcome the denaturation of protein and sticky blood cell separation. Hemolysis may happen because of the presence of the pump. Here, blood circulation is monitored by adapting a pump	82

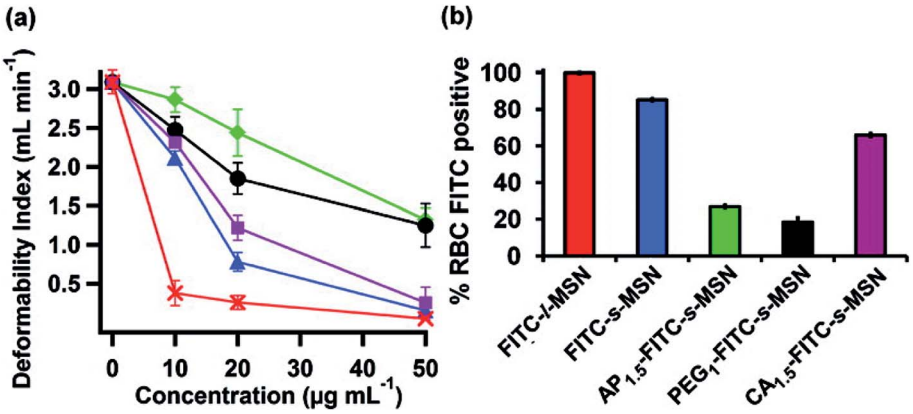

Fig. 5 (a) Deformability Index (DI) of RBCs incubated with s-MSN (blue), AP1.5-s-MSN (green), PEG1-s-MSN (black), CA1.5-s-MSN (purple), and l-MSN (red). (b) Flow cytometry analyses of RBCs incubated with FITC-l-MSN (red), FITC-s-MSN (blue), AP1.5-FITC-s-MSN (green), PEG1-FITC-s-MSN (black), and CA1.5-FITC-s-MSN (purple). Reproduced with permission from ref. 6. Copyright © 2011 American Chemical Society.

Shinto *et al.* selected a different size range of silica nanoparticles (28, 50, 55, 156, and 461 nm) and performed the hemolysis assay (4 h). The result indicated that the smaller size silica nanoparticles with high nanoparticles mass dose demonstrate inclined hemolysis activity. Regardless of the nanoparticle diameter, the size- and dose-dependent hemolytic action of the silica nanoparticles seemed to be depicted by a master curve as a function of the nanoparticle surface area per suspension volume[91] at various concentrations (0, 10, 20, 50, and 100 μg ml^{-1}) and times (30 min, 2 h). Silica nanoparticles with a diameter of 58 nm depicted a dose-dependent hemolysis activity, and also the higher the malondialdehyde (MDA) the lower the superoxide dismutase (SOD) efficacy. Hence, it enhances the oxidative injury in RBCs.[92]

To understand the effect of particle size in the hemocompatibility of MSNs, Zhao *et al.* studied the interactions of the two most familiar types of MSNs (MCM-41 and SBA-15) accompanied by red blood cells (RBCs). As claimed by their study, small MCM-41-type MSNs adsorbed to the surface of RBCs but did not cause any disturbance to the morphology or membranes. However, significant changes and membrane deformation were found when the adsorption of large SBA-15-type MSNs took place at RBC surface that finally causes hemolysis.[6]

They also stated a pair of chief processes that are responsible for the reciprocal action between MSN and RBC membranes: (1) establishment of a bond between silanol-rich MSN surfaces and RBC membranes enriched with phosphatidyl choline[93] and (2) bending of the RBC membrane to tailor to the rigid surface of MSNs.[94–98] The interactions mainly happen when the required quantity of free energy is available to bend the membrane and adapt to the surface of MSNs.[6] They not only studied the effect of the particle size and surface area on the hemolytic properties of MSNs but also concentrated on how chemical characteristics and the degree of surface modification of particle effect the interactions with RBCs. This knowledge will help us to rationally design biocompatible particles and restrain the spreading of MSNs in the bloodstream.

4.2.2. Particle morphology and surface modification. Different studies have already revealed the influence of morphology and surface functionalization of MSNs on the hemolytic activity. According to Yu *et al.*, the shape and surface charge of MSNs have a great impact on the hemolytic business with RBCs. In their research, they have chosen mesoporous silica nanospheres, having a diameter of 120 nm with an aspect ratio of 2, 4 and 8 (width by length 80 × 200 nm, 150 × 600 nm and 130 × 1000 nm, respectively). Therefore, their surface was modified with primary amine silane groups to produce positive charge and render them cationic in nature. Thereafter, they were evaluated with human erythrocytes, macrophages and lung cancer cells. The outcome of this study tells us about the fact that for bare MSNs, the hemolytic activity was porosity and geometry dependent and for amine-modified MSNs, it was surface-charge dependent.[99] This study provided us with another important information that the morphology of MSNs had no impact on the hemolytic activity with human red blood cells up to a concentration of 100 mg ml^{-1}.[100] This study clearly stated the lower hemolytic efficacy (5–30%) of greater aspect ratio MSNs rather than spherical and smaller aspect ratio MSNs (50–90%).[99]

To set up the effect of different morphologies on the hemolytic activity of MSNs with human erythrocytes, Joglekar *et al.*[111] implemented an experiment. In their experiment, they have chosen four different types of MSNs, namely, large spherical (LS), small spherical (SS), large tubular (LT) and small tubular (ST) MSNs. The preliminary hemolytic assay of four different types of MSNs (LS, SS, LT, and ST) was performed by incubating human red blood cells with each of the above-mentioned MSNs at diverse concentrations at room temperature for 2, 4 and 8 h. After incubation, the samples were centrifuged at 345 × *g* for 5 minutes to ensure visual perception and quantitative estimation of the hemoglobin present in the supernatant. The absorbance of the supernatant was determined at 541 nm to measure the extent of hemoglobin released and also the percent hemolysis done as per the method demonstrated by Zhao *et al.*[6] Formerly mentioned four different

types of MSNs exhibited lower hemolytic activity at concentrations of 20, 50 and 100 mg ml^{-1}. The hemolytic assay result was consistent with the previous result obtained by Yu *et al.* So, it was shown that all different types of MSN morphologies exhibited hemocompatibility up to concentrations of 100 mg ml^{-1}, and the geometry did not play any role in the blood biocompatibility. Finally, after evaluating the results obtained from primary hemolytic assay it can be said that the spherical geometry (MSNs) is more hemocompatible than their tubular geometry counterparts. Above studies give us profound knowledge on how to design more critical and hemocompatible MSN-based drug delivery carriers with different morphologies for more accurate implementation.

Roggers *et al.* were able to minimize the hemolytic effect of large-pore MSNs (l-MSNs) by external surface modification with the lipid bilayer. This lipid bilayer modification is not only an indication of healthy RBCs but also capable of lowering speculation harm to RBCs. The result of this research is that lipid-bilayer-covered l-MSNs show significantly lower hemolytic activity to the outer membrane of RBCs, and these data will help in the future to fabricate MSN-based novel drug delivery systems.[101] Surface modification can be applied to mask the MSN surface to reduce the interactions with trimethyl ammonium groups of the RBC membranes. This technique helps to inhibit the hemolytic effect. Ethylene groups on the surface of the MSNs could also reduce the hemolysis.[102]

4.2.3. Surface roughness. Surface roughness is one of the notable parameters of MSNs, which has a significant impact on the hemolytic activity. It helps to define the relationship between different parameters of nanomaterials with surface structure. Surface roughness can be observed in the outermost surface of a particle as generally happens with digs, pits, scratches, polishing marks, dust particles, granules, crystals, *etc.* (Bennett and Mattsson, 1989).[113] It is very tough to determine the surface roughness by itself, but there is a mathematical character named surface fractal dimensions (Ds) that help to correlate surface roughness within a certain range.

Divergent size and shape of porous structures and various degrees of crosslinking among itself influence the significant hallmarks and hydrothermal resistance of MSNs. Impregnation of the outermost wall of the MSNs by active metal compounds (Al and Cu) is a recent advancement in the field of MSN-based drug delivery systems to reduce the deleterious effect of nanoparticles on biological systems.[103]

This study shed light on the bridge between various hydrothermal resistances of MSNs such as HMS, MSU, MCM, and SBA families of silica and surface roughness. Here, HMS (hollow mesoporous silica) and MSU (Michigan State University) silica (made from Tergitol and Tween surfactants) with the lowest surface roughness show higher hydrothermal and mechanical resistance.[104] This hydrothermal resistance improves the stability of MSNs, which has further relation with hemocompatibility.

Another research detailed that pegylated mesoporous silica (PEG-MSNs) exhibits more hemocompatibility, reduces the uptake of macrophage and thus makes it a popular candidate for drug delivery. They have taken hydrothermally treated pegylated MSNs (<50 nm) for this study. Pegylated MSNs demonstrate high stability at both physiological and room temperatures. Hemolysis study confirms that there are no significant changes observed in RBCs after 24 hours of exposure at a comparatively higher concentration (1000 μg ml^{-1}).[105]

4.3. Influence of protein corona (PC) interaction on hemolysis

As MSNs exhibit hemolytic and cytotoxic properties, there were plenty of measures that have been adopted by scientists to mitigate the unwanted effect of MSNs as nanocarriers.[106] Protein corona interaction is one of the pivotal parameters

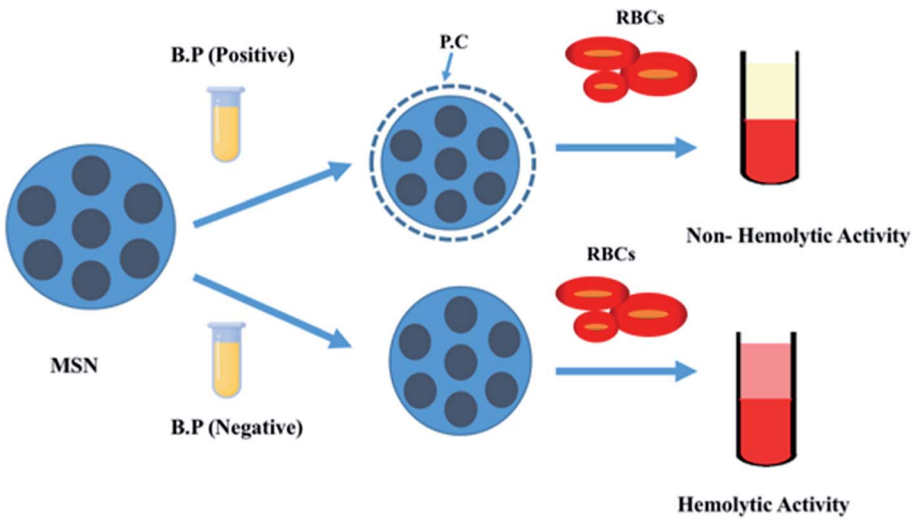

Fig. 6 Effect of Protein-corona (P.C.) on the hemolytic activity of MSNs. This schematic shows that P.C. is formed on the surface of MSNs in the presence of Blood Plasma (B.P.) [B.P.: positive] and not formed in the absence of blood plasma [B.P.: negative]. This P.C. formation further prevents the interaction of MSNs with RBCs and thus reduces the hemolysis.

when we consider MSN interaction with blood. Protein corona is a steady biomolecule covering formed by the adsorption of plasma biomolecules on the uppermost layer of the nanoparticles.[107,108] Paula *et al.*[112] in their paper described that MSNs less than a hundred nanometers in size with three different surface electrochemical and micro chemical features do not exhibit hemolytic activity on RBCs. This experiment was performed in the presence of human blood plasma. However, in the presence of phosphate buffer solution, significant hemolytic activity was observed.

For this experiment, three surface-modified nanoparticles (Si–OH, Si–NH_2, and Si–P $(CH_3)_3O_3H$) with five different concentrations (32.2, 62.5, 125, 250, and 500 μg ml^{-1}) were taken. Deionized water and phosphate buffer solution (PBS) were considered as positive and negative controls, respectively. Toxicity showed dose dependency when the experiment was performed in the presence of PBS, equal to the highest

Table 2 Summary of the influences of various types of MSN characteristics on hemolysis

	Type	Surface modification	Outcome	Reason	Ref.
Size based	25–225 nm	—	Size and dose-dependent hemolytic activity (H.A.)	Small MSN-25 has greater than expected pore size and primary pore volume	27
	MCM-41 AND SBA-15	—	MCM-41 shows lower H.A.	Interaction due to the production of the bond between MSN surface and RBC membrane	110
			SBA-15 shows H.A.	RBC membrane bowing to customize the tough surface of MSNs	
Particles morphology and surface modification	Mesoporous silica nanorods (120 nm diameter, aspect ratio: 2, 4 and 8)	Primary amine silane group	Bare MSNs: H.A. is porosity- and geometry-dependent Amine modified MSNs: H.A. is surface charged dependent H.A. independent on MSN morphologies (up to concentration 100 mg ml^{-1}) Greater aspect ratio MSNs: low H.A. Spherical and lower aspect ratio MSNs: high H.A.	—	99
	Four different types of MSNs LS, SS, LT, ST		At a concentration of 20, 50 and 100 mg ml^{-1} lower H.A. observed for four different types of MSNs Spherical geometry MSNs: more hemocompatible Tubular geometry MSNs: less hemocompatible	—	111
	Large pore MSNs (l-MSNs)	Lipid bi-layer	Indicate the health of RBCs Reduce speculation hazards to RBCs Lower H.A. In the presence of phosphate buffer solution (PBS) and human blood plasma: no hemolysis	—	101
Surface roughness	HMS, MSU, MCM, SBA	—	HMS and MSU show comparatively higher hemocompatibility	Both have the lowest surface roughness and higher hydrothermal and mechanical resistance	104
Protein-corona interaction	MSNs (<100 nm in size)	Three different functional groups [–OH, –NH_2, –$P(CH_3)_3OH$]	In the presence of phosphate buffer solution (PBS) and human blood plasma: no hemolysis	Surface modification (–NH_2)	112
			PBS without human blood plasma: hemolysis	Formation of PC	
			–NH_2 modified MSNs: lower H.A.		

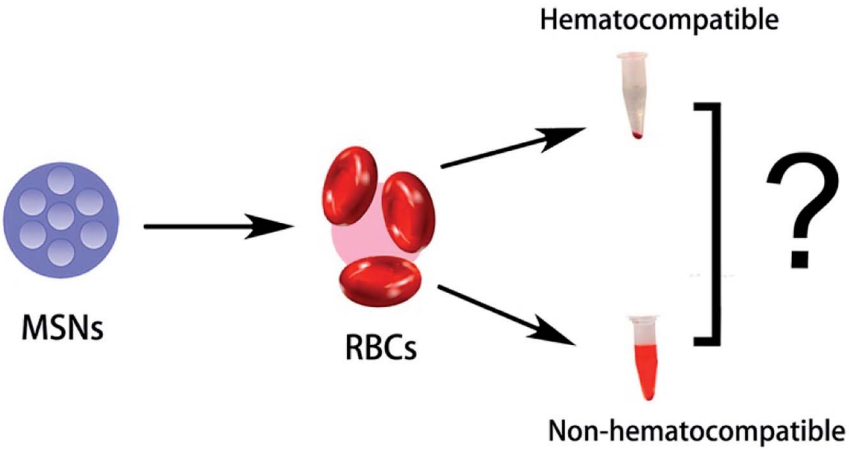

Fig. 7 Diagrammatic representation of MSN hemocompatibility with RBCs.

concentration adopted in this study (500 μg ml^{-1}). Silanol groups (Si–OH) were abundantly present on the surface of the nanoparticles. They are mainly responsible accounting for greater than 50% of RBC destructions in the solution. Ammonia-modified mesoporous silica nanoparticles (Si–NH_2) possess the lowest cytotoxic property, nearly about 10% of hemolysis.

However, no hemolysis occurred for all samples and all concentrations tested in a PBS solution that contained human blood plasma (even at low concentrations of plasma-like 2%). Another reason behind the lack of hemolysis was the formation of hard corona silica nanoparticles after incubation with 55% of plasma.[109] So, this study revealed some knowledge about the formation of Protein corona and their interaction with nanoparticles, which could further lead to the formation of a robust outer cover onto the surface of the nanoparticles. That corona formation will isolate the surface micro chemical environment and other biochemical properties of the surface groups (silanol, amine and methylphosphonate). Thus, it will help to abate the hemolytic effect of MSNs with RBCs (Fig. 6 and Table 2).

5. Conclusions

The main objective of this review is to provide insights into the hemocompatibility of MSNs, along with its synthetic procedure and applications described in a healthy manner. There are a lot of studies present that demonstrated the hemolytic effect of MSNs and possible solutions. However, a lack of much valuable information regarding the hemocompatibility of MSNs has been noticed. The lack of knowledge is due to a few separate studies done with physicochemical properties of MSNs. Therefore, it is not very easy to conclude very distinctively.

Various synthesis processes and influences of different characters of MSNs, such as shape, size, surface morphology, surface chemistry, surface modification, surface roughness, and protein corona interaction (by many scientists across the globe) are well elaborated. The initial discussion about the different types of preparation methods for MSNs such as Stober's method, sol–gel technique, and swelling–shrinking mechanism has been done, and their potential application in the different biomedical arena were further focused. Further elaboration continues about the effect of the MSN size on the hemolytic activity towards human red blood cells. In that context, it is noticeable that the size and dose relying on the toxicity of MSNs and hemocompatibility are directly proportional to the particle size (MSN-25 shows low hemolytic efficacy). In another study, they carried out the hemolytic study among two prominent types of MSNs, such as small MSN-41 and large SBA-15. Small MSN-41 showed no disturbance or toxicity towards the surface of RBCs, whereas sizeable SBA-15-type MSNs revealed hemolytic activity.

Here the effect of surface morphologies, chemical modifications and surface roughness on the hemolytic activity of MSNs is also emphasized. From the study conducted by Joglekar *et al.*, relevant information can be gained that concentrations up to 100 mg ml^{-1} of various kinds of MSNs demonstrated hemocompatibility, and it was geometry independent. At the end, it is obvious that the spherical geometry possesses relatively more hemocompatibility rather than the tubular geometry. Another study revealed that the hemolytic activity depended on the porosity and geometry in case of bare MSNs, but surface charge hooked for amine-functionalized MSNs.

Protein Corona Interaction (PCI) is one of the significant parameters that we have taken into our consideration. PCI is a new idea where MSNs interact with blood plasma and form a rigid cover onto the surface of RBCs, which further leads to the prevention of the interactions between MSNs and RBCs. Thus, it reduced the hemolytic activity. According to the study conducted by Paula *et al.*, MSN size range less than 100 nm and three distinct surface electrochemical and microchemical properties do not demonstrate hemolytic feature towards human RBCs in the presence of human blood plasma. However, noticeable hemolysis was observed in the study done in the media that contained phosphate buffer solution. However, there is a lack of data that can ensure the exact mechanism underlying the interactions between MSNs and RBCs in the presence of a biological atmosphere, which further leads to the formation of the protein corona. If it is possible to solve the

issues related to the hemolytic effect of MSNs on RBCs by adapting newer technologies or modifications, MSNs will be the most promising candidate for the nano-drug delivery system.

According to our view, rather than other characteristics such as shape, size, dose, and surface charge, mesoporosity is the critical structural property of MSNs that play a pivotal role in the context of biological activities of these nanomaterials (Fig. 7).

6. Future perspectives

In our opinion, increasing studies should be conducted to ensure MSNs as safe nanocarriers towards novel drug delivery systems. To ensure hemocompatibility, many biological studies should be carried out in well-founded and suitable biological milieu. We can also do extensive research by altering the physicochemical features of MSNs to ensure MSNs as hemocompatible nanocarriers. It is necessary to know the proper effect of surface silanol groups and surface morphology on the interactions of MSNs with biological systems. In our view, it is also imperative to establish the appropriate mechanism underlying the formation of protein corona and find the possible coating method that can prohibit the interactions between MSNs and RBCs in biological media and can thus reduce the hemolytic activity of MSNs. Also, changing the synthesis method, structural changes or chemical modification can reduce or stop the hemolytic activity of MSNs. Our aspiration for this article is that it can give us understandable knowledge of possible causes related to MSN hemolytic activity and progress that has already done in this field over the past few years and also give us feasible studies that should be enacted in the future to make MSNs more hemocompatible.

Conflicts of interest

The authors declare no conflicts of interest.

Acknowledgements

This work was supported by the Double First-Class Innovation Team of China Pharmaceutical University (CPU2018GY40).

References

1 D. S. T. Martinez, A. J. Paula, L. C. Fonseca, L. A. V. Luna, C. P. Silveira, N. Duran and O. L. Alves, *Eur. J. Inorg. Chem.*, 2015, 4595–4602.
2 S. Gordon, E. Teichmann, K. Young, K. Finnie, T. Rades and S. Hook, *Eur. J. Pharm. Sci.*, 2010, **41**, 360–368.
3 M. Joglekar, R. A. Roggers, Y. Zhao and B. G. Trewyn, *RSC Adv.*, 2013, **3**, 2454–2461.
4 J. Zhang, Y. Sun, B. Tian, K. Li, L. Wang, Y. Liang and J. Han, *Colloids Surf., B*, 2016, **144**, 293–302.
5 A. S. Wani, *Formulation Development of Mesoporous Silica Nanoparticles as an Injectable Delivery System*, Wayne State University, 2013, p. 713.
6 Y. Zhao, X. Sun, G. Zhang, B. G. Trewyn, I. I. Slowing and V. S.-Y. Lin, *ACS Nano*, 2011, **5**, 1366–1375.
7 M. Zhu, Y. Zhu, L. Zhang and J. Shi, *Sci. Technol. Adv. Mater.*, 2013, **14**, 045005.
8 S. Kwon, R. K. Singh, R. A. Perez, E. A. Abou Neel, H. W. Kim and W. Chrzanowski, *J. Tissue Eng.*, 2013, **4**, 2041731413503357.
9 M. Liong, J. Lu, M. Kovochich, T. Xia, S. G. Ruehm, A. E. Nel, F. Tamanoi and J. I. Zink, *ACS Nano*, 2008, **2**, 889–896.
10 T. Asefa and Z. Tao, *Chem. Res. Toxicol.*, 2012, **25**, 2265–2284.
11 T. Yanagisawa, T. Shimizu, K. Kuroda and K. Chuzo, *Bull. Chem. Soc. Jpn.*, 1990, **63**, 988–992.
12 Z. Tao, M. P. Morrow, T. Asefa, K. K. Sharma, C. Duncan, A. Anan, H. S. Penefsky, J. Goodisman and A.-K. Souid, *Nano Lett.*, 2008, **8**, 1517–1526.
13 D. Tarn, C. E. Ashley, M. Xue, E. C. Carnes, J. I. Zink and C. J. Brinker, *Acc. Chem. Res.*, 2013, **46**, 792–801.
14 W. Stöber, A. Fink and E. Bohn, *J. Colloid Interface Sci.*, 1968, **26**, 62–69.
15 M. Grün, I. Lauer and K. K. Unger, *Adv. Mater.*, 1997, **9**, 254–257.
16 J.-L. Blin and M. Impéror-Clerc, *Chem. Soc. Rev.*, 2013, **42**, 4071–4082.
17 C. Gao, H. Qiu, W. Zeng, Y. Sakamoto, O. Terasaki, K. Sakamoto, Q. Chen and S. Che, *Chem. Mater.*, 2006, **18**, 3904–3914.
18 K. Flodström, H. Wennerström and V. Alfredsson, *Langmuir*, 2004, **20**, 680–688.
19 G. S. Attard, J. C. Glyde and C. G. Göltner, *Nature*, 1995, **378**, 366.
20 A. Sundblom, C. L. Oliveira, A. E. Palmqvist and J. S. Pedersen, *J. Phys. Chem. C*, 2009, **113**, 7706–7713.
21 J. S. Beck, J. Vartuli, W. J. Roth, M. Leonowicz, C. Kresge, K. Schmitt, C. Chu, D. H. Olson, E. Sheppard and S. McCullen, *J. Am. Chem. Soc.*, 1992, **114**, 10834–10843.
22 C. Kresge, M. Leonowicz, W. J. Roth, J. Vartuli and J. Beck, *nature*, 1992, **359**, 710.
23 M. J. Hollamby, D. Borisova, P. Brown, J. Eastoe, I. Grillo and D. Shchukin, *Langmuir*, 2011, **28**, 4425–4433.
24 K. J. Edler, *Aust. J. Chem.*, 2005, **58**, 627–643.
25 Z. Yi, L. F. Dumée, C. J. Garvey, C. Feng, F. She, J. E. Rookes, S. Mudie, D. M. Cahill and L. Kong, *Langmuir*, 2015, **31**, 8478–8487.
26 R. Narayan, U. Nayak, A. Raichur and S. Garg, *Pharmaceutics*, 2018, **10**, 118.
27 Y.-S. Lin and C. L. Haynes, *J. Am. Chem. Soc.*, 2010, **132**, 4834–4842.
28 S. Williams, A. Neumann, I. Bremer, Y. Su, G. Dräger, C. Kasper and P. Behrens, *J. Mater. Sci.: Mater. Med.*, 2015, **26**, 5409.
29 J. L. Blin, F. Michaux and M. J. Stébé, *Colloids Surf., A*, 2016, **510**, 104–112.
30 D. Brevet, C. Jouannin, C. Tourné-Péteilh, J.-M. Devoisselle, A. Vioux and L. Viau, *RSC Adv.*, 2016, **6**, 82916–82923.
31 S. Kwon, R. Singh, R. Perez, E. Abou Neel, H.-W. Kim and W. Chrzanowski, *J. Tissue Eng.*, 2013, **4**, 2041731413503357.
32 S. R. Abd Shukor, N. A. Zainal, H. Wab and K. Razak, *Chemical Engineering Transactions*, 2013, **32**, 2245–2250.

33 H. Mekaru, A. Yoshigoe, M. Nakamura, T. Doura and F. Tamanoi, *ACS Appl. Nano Mater.*, 2019, **2**, 479–488.
34 X. Du, F. Kleitz, X. Li, H. Huang, X. Zhang and S.-Z. Qiao, *Adv. Funct. Mater.*, 2018, 1707325.
35 M. Quesada, C. Muniesa and P. Botella, *Chem. Mater.*, 2013, **25**, 2597–2602.
36 Y.-L. Luo, X.-C. Huang, W.-M. Tu and H.-Y. Hsu, *Anal. Chim. Acta*, 2016, **902**, 196–204.
37 O. Pagar, H. Nagare, Y. Chine, R. Autade, P. Narode and V. Sanklecha, *Journal of Pharmaceutics and Drug Analysis*, 2018, **6**, 1–12.
38 Z. Qiao, L. Zhang, M. Guo, Y. Liu and Q. Huo, *Chem. Mater.*, 2009, **21**, 3823–3829.
39 K. Moeller, J. Kobler and T. Bein, *Adv. Funct. Mater.*, 2007, **17**, 605–612.
40 S. A. El-Safty and J. Evansb, *J. Mater. Chem.*, 2002, **12**, 117.
41 P. Feng, X. Bu and D. J. Pine, *Langmuir*, 2000, **16**, 5304–5310.
42 L. Bronstein, E. Krämer, B. Berton, C. Burger, S. Förster and M. Antonietti, *Chem. Mater.*, 1999, **11**, 1402–1405.
43 D. Zhao, Q. Huo, J. Feng, B. F. Chmelka and G. D. Stucky, *J. Am. Chem. Soc.*, 1998, **120**, 6024–6036.
44 Y. Kamari and M. Ghiaci, *Microporous Mesoporous Mater.*, 2016, **234**, 361–369.
45 R. Richer, *Chem. Commun.*, 1998, 1775–1777.
46 I. I. Slowing, J. L. Vivero-Escoto, B. G. Trewyn and V. S. Y. Lin, *J. Mater. Chem.*, 2010, **20**, 7924–7937.
47 Y. A. Shchipunov and T. y. Y. Karpenko, *Langmuir*, 2004, **20**, 3882–3887.
48 S. Rahmani, J. Budimir, M. Sejalon, M. Daurat, D. Aggad, E. Vives, L. Raehm, M. Garcia, L. Lichon, M. Gary-Bobo, J.-O. Durand and C. Charnay, *Molecules*, 2019, **24**, 332.
49 M. Sevilla and A. B. Fuertes, *Chem. Phys. Lett.*, 2010, **490**, 63–68.
50 M.-H. Kim, H.-K. Na, Y.-K. Kim, S.-R. Ryoo, H. S. Cho, K. E. Lee, H. Jeon, R. Ryoo and D.-H. Min, *ACS Nano*, 2011, **5**, 3568–3576.
51 E. Yamamoto, S. Mori, A. Shimojima, H. Wada and K. Kuroda, *Nanoscale*, 2017, **9**, 2464–2470.
52 J. Yi and M. Kruk, *Langmuir*, 2015, **31**, 7623–7632.
53 J. Fan, G. Fang, X. Wang, F. Zeng, Y. Xiang and S. Wu, *Nanotechnology*, 2011, **22**, 455102.
54 M. Liong, J. Lu, M. Kovochich, T. Xia, S. G. Ruehm, A. E. Nel, F. Tamanoi and J. I. Zink, *ACS Nano*, 2008, **2**, 889–896.
55 B. G. Trewyn, S. Giri, I. I. Slowing and V. S.-Y. Lin, *Chem. Commun.*, 2007, 3236–3245.
56 I. I. Slowing, J. L. Vivero-Escoto, C.-W. Wu and V. S.-Y. Lin, *Adv. Drug Delivery Rev.*, 2008, **60**, 1278–1288.
57 M. Manzano, M. Colilla and M. Vallet-Regí, *Expert Opin. Drug Delivery*, 2009, **6**, 1383–1400.
58 J. L. Vivero-Escoto, I. I. Slowing, B. G. Trewyn and V. S. Y. Lin, *Small*, 2010, **6**, 1952–1967.
59 S. Yi, M. L. Miller and A. J. D. Pasqua, *Comments Inorg. Chem.*, 2015, **36**, 61–80.
60 W. van Oeveren, *Scientifica*, 2013, **2013**, 392584.
61 M. Carme Coll Ferrer, U. N. Eckmann, R. J. Composto and D. Eckmann, *Toxicol. Appl. Pharmacol.*, 2013, 703–712.
62 S. Blok, G. Engels and W. Oeveren, *Biointerphases*, 2016, **11**, 029802.
63 X. Punet, R. Mauchauffé, J. Rodríguez-Cabello, M. Alonso, E. Engel and M. Mateos-Timoneda, *Regener. Biomater.*, 2015, 167–175.
64 C. C. mohan, K. Chennazhi and D. Menon, *Acta Biomater.*, 2013, 9568–9577.
65 C. L. Haycox and B. D. Ratner, *J. Biomed. Mater. Res.*, 1993, **27**, 1181–1193.
66 U. Streller, C. Sperling, J. Hübner, R. Hanke and C. Werner, *J. Biomed. Mater. Res., Part B*, 2003, 379–390.
67 M. F. Maitz, C. Sperling, T. Wongpinyochit, M. Herklotz, C. Werner and F. P. Seib, *Nanomedicine*, 2017, **13**, 2633–2642.
68 M. Sanak, B. Jakieła and W. Węgrzyn, *Bulletin of the Academy of Sciences, Technical Sciences*, 2010, **58**(2), 317–322.
69 R. Van Kruchten, J. M. E. M. Cosemans and J. W. M. Heemskerk, *Platelets*, 2012, **23**, 229–242.
70 J. M. Lackner, W. Waldhauser, P. Hartmann, F. Bruckert, M. Weidenhaupt, R. Major, M. Sanak, M. Wiesinger and D. Heim, *J. Funct. Biomater.*, 2012, **3**(2), 283–297.
71 W. G. McClung, D. Babcock and J. Brash, *J. Biomed. Mater. Res., Part A*, 2007, **81**(3), 644–651.
72 S. Krajewski, R. Prucek, A. Panacek, M. Avci-Adali, A. Nolte, A. Straub, R. Zboril, H. P. Wendel and L. Kvitek, *Acta Biomater.*, 2013, **9**, 7460–7468.
73 K. Stang, S. Krajewski, B. Neumann, J. Kurz, M. Post, S. Stoppelkamp, S. Fennrich, M. Avci-Adali, D. Armbruster, C. Schlensak, I. A. Burgener, H. P. Wendel and T. Walker, *Mater. Sci. Eng., C*, 2014, **42**, 422–428.
74 M. Mueller, B. Krolitzki and B. Glasmacher, in *Biomedical Engineering/Biomedizinische Technik*, 2012, vol. 57, p. 549.
75 S. Nordling, B. Nilsson and P. Magnusson, *J. Visualized Exp.*, 2014, **93**, 52112.
76 N. Kent, L. Basabe-Desmonts, G. Meade, B. Maccraith, B. Corcoran, D. Kenny and A. Ricco, *Biomed. Microdevices*, 2010, **12**, 987–1000.
77 A. A. Onasoga-Jarvis, K. Leiderman, A. L. Fogelson, M. Wang, M. J. Manco-Johnson, J. A. Di Paola and K. B. Neeves, *PLoS One*, 2013, **8**, e78732.
78 A. A. Onasoga-Jarvis, T. J. Puls, S. K. O'Brien, L. Kuang, H. J. Liang and K. B. Neeves, *J. Thromb. Haemostasis*, 2014, **12**, 373–382.
79 K. M. Kovach, J. R. Capadona, A. S. Gupta and J. A. Potkay, *J. Biomed. Mater. Res., Part A*, 2014, **102**, 4195–4205.
80 S. Zhu, B. A. Herbig, R. Li, T. V. Colace, R. W. Muthard, K. B. Neeves and S. L. Diamond, *Biorheology*, 2015, **52**, 303–318.
81 M. Nagy, J. W. M. Heemskerk and F. Swieringa, *Platelets*, 2017, **28**, 441–448.
82 W. Oeveren, I. Tielliu and J. de Hart, *Int. J. Biomater.*, 2012, **2012**, 673163.
83 M. Weber, H. Steinle, S. Golombek, L. Hann, C. Schlensak, H. P. Wendel and M. Avci-Adali, *Frontiers in Bioengineering and Biotechnology*, 2018, **6**, 99.

84 Q. Qian, K. A. Nath, Y. Wu, T. M. Daoud and S. Sethi, *Am. J. Kidney Dis.*, 2010, **56**, 780–784.
85 É. Biró, K. N. Sturk-Maquelin, G. M. T. Vogel, D. G. Meuleman, M. J. Smit, C. E. Hack, A. Sturk and R. Nieuwland, *J. Thromb. Haemostasis*, 2003, **1**, 2561–2568.
86 J. W. Kuhbier, V. Coger, J. Mueller, C. Liebsch, F. Schlottmann, V. Bucan, P. M. Vogt and S. Strauss, *J. Mater. Sci.: Mater. Med.*, 2017, **28**, 127.
87 B. Neun and M. A. Dobrovolskaia, *Method for Analysis of Nanoparticle Hemolytic Properties In Vitro*, 2011.
88 G. Totea, D. Ionita, I. Demetrescu and M. Magdalena Mitache, *Cent. Eur. J. Chem.*, 2014, **12**, 796–803.
89 S. S. Hall, S. Mitragotri and P. S. Daugherty, *Biotechnol. Prog.*, 2007, **23**, 749–754.
90 H. Reid, A. Barnes, P. Lock, J. Dormandy and T. Dormandy, *J. Clin. Pathol.*, 1976, **29**, 855.
91 H. Shinto, T. Fukasawa, K. Yoshisue, M. Tezuka and M. Orita, *Adv. Powder Technol.*, 2014, **25**, 1872–1881.
92 L. Jiang, Y. yu, Y. Li, Y. Yu, J. Duan, Y. Zou, Q. Li and Z. Sun, *Nanoscale Res. Lett.*, 2016, 11.
93 I. I. Slowing, C. W. Wu, J. L. Vivero-Escoto and V. S. Y. Lin, *Small*, 2009, **5**, 57–62.
94 M. Deserno and W. M. Gelbart, *J. Phys. Chem. B*, 2002, **106**, 5543–5552.
95 B. J. Reynwar, G. Illya, V. A. Harmandaris, M. M. Müller, K. Kremer and M. Deserno, *Nature*, 2007, **447**, 461.
96 C. C. Fleck and R. Netz, *EPL*, 2004, **67**, 314.
97 Y. Roiter, M. Ornatska, A. R. Rammohan, J. Balakrishnan, D. R. Heine and S. Minko, *Nano Lett.*, 2008, **8**, 941–944.
98 R. Lipowsky and H.-G. Döbereiner, *EPL*, 1998, **43**, 219.
99 T. Yu, A. Malugin and H. Ghandehari, *ACS Nano*, 2011, **5**, 5717–5728.
100 T.-W. Kim, I. I. Slowing, P.-W. Chung and V. S.-Y. Lin, *ACS Nano*, 2010, **5**, 360–366.
101 R. A. Roggers, M. Joglekar, J. S. Valenstein and B. G. Trewyn, *ACS Appl. Mater. Interfaces*, 2014, **6**, 1675–1681.
102 F. Farjadian, A. Roointan, S. Mohammadi Samani and M. Hosseini, *Chem. Eng. J.*, 2019, **359**, 684–705.
103 R. K. Kankala, H. Zhang, L. chen-guang, K. Kanubaddi, C.-H. Lee, W. Cui, H. Santos, K. Lin and A.-Z. Chen, *Adv. Funct. Mater.*, 2019, **29**, 1902652–1902694.
104 E. Prouzet, C. Boissière, S. S. Kim and T. J. Pinnavaia, *Microporous Mesoporous Mater.*, 2009, **119**, 9–17.
105 Y.-S. Lin, N. Abadeer and C. Haynes, *Chem. Commun.*, 2010, **47**, 532–534.
106 L. A. Torre, R. Siegel, E. M. Ward and A. Jemal, *Cancer Epidemiol., Biomarkers Prev.*, 2015, **25**, 16–27.
107 T. Cedervall, I. Lynch, M. Foy, T. Berggård, S. C. Donnelly, G. Cagney, S. Linse and K. A. Dawson, *Angew. Chem., Int. Ed.*, 2007, **46**, 5754–5756.
108 M. Lundqvist, J. Stigler, G. Elia, I. Lynch, T. Cedervall and K. A. Dawson, *Proc. Natl. Acad. Sci. U. S. A.*, 2008, **105**, 14265–14270.
109 A. J. Paula, D. S. T. Martinez, R. T. Araujo Júnior, A. G. Souza Filho and O. L. Alves, *J. Braz. Chem. Soc.*, 2012, **23**, 1807–1814.
110 Y. Zhao, X. Sun, G. Zhang, B. G. Trewyn, I. I. Slowing and V. S. Y. Lin, *ACS Nano*, 2011, **5**, 1366–1375.
111 M. Joglekar, R. Roggers, Y. Zhao and B. Trewyn, *RSC Adv.*, 2013, **3**, 2454–2461.
112 A. Paula, D. Martinez, R. Araujo, A. Filho and O. Alves, *J. Braz. Chem. Soc.*, 2012, **23**, 1807–1814.
113 J. M. Bennett and L. Mattsson, *Introduction to Surface Roughness and Scattering*, Optical Society of America, 1999.